CARCASS DEFLECTION ANALYSIS ON A TURBO-FAN ENGINE

O. FUNATOGAWA

T. INOUE

T. OHNO

Civil Aero-Engine Development Dept.

Aero-Engine & Space Operations

Ishikawajima-Harima Heavy Industries Co., Ltd.

SUMMARY

The use of NASTRAN in carcass deflection analysis on a turbo-fan engine is described. The main purpose of the analysis in an early stage of a new engine development is to optimize engine geometrical configurations from the viewpoint of engine performance. Engine structural memebers are replaced by a mathematical model and NASTRAN input data is generated by an in-house pre-processor SANA/MESH. Some static analysis results are presented.

INTRODUCTION

Carcass deflection analysis using an overall engine structural model is necessary for a new engine development. In the early stage of development, the model is not so accurate because it is made from a preliminary design scheme. This model is refined based on experimental results of engine compornent as well as overall mechnical rig tests.

The main purpose of the analysis is to find the optimum engine geometrical configuration including an engine mount system, a bearing support system and stiffness distribution of casings and rotors, with respect to engine performance, and to feed it back to the design scheme. Engine performance deterioration depending on tip clearance increase dur to rubbing between the rotors and casings is estimated by calculating casing relative deformation to the rotor. The analytical investigation of the engine performance deterioration problem has been reported by E.G. Stakolish. (1) (2)
Second, an overall engine model analysis under various load conditions provides internal load. Then a detail stress analysis of each component model is carried out using the internal load as a boundary condition.
Third, the overall model is available for a dynamic analysis, in which a coupling effect with an airframe structure is especially important.
This kind of dynamic problem has been collaborated by Boeing Commercial Airplane Company and Pratt & Whitney Aircraft. (3)
In this paper, engine structure is modeled on the design scheme of a new turbo-fan engine which is being developed by United Kingdom and Japanese jet engine manufacturers. NASTRAN has been used in this calculation in IHI because of it's wide applicability, high reliability and common availability. J. L. White and D. L. Baste have reported the NASTRAN application to this kind of problem at the 4th users' conference. (4)

STRUCTURE MODEL

The turbo-fan engine, as shown in Fig. 1, can be divided into five principal components: fan and low pressure compressor, high pressure compressor, combustor, high pressure turbine and low pressure turbine.

The nacelle, including intake, fan cowling, fan duct and nozzle, and core cowling and nozzle, is a boundary portion between an airframe and an engine manufacturer.

Most of the nacelle structures are not considered in the primary stage of this kind of analysis.

An intermediate casing, which consists of a fan frame and a front bearing support structure, and a turbine bearing support structure are important members to connect casings and rotors.

The engine itself is supported by an airframe pylon with front and rear mount links.

The engine was modeled and input BULK DATA was made in the following procedure. Main grid points on the casing longitudinal section were defined, and BULK DATA of cylindrical casings and struts were generated by using the in-house pre-processor SANA/MESH considering axial and cyclic symmetry. Casings were modeled with QUAD4 and TRIA3 shell elements divinding 16 pieces circumferentialy. Flanges and circumferential stiffeners on the casing were modeled with off-set BAR elements. Intermediate casing struts, which had a hollow section with internal ribs, were modeled with the combination of BAR elements and QUAD4 elements with independent in-plane and out-of-plane shell stiffness in order to achieve equivalent section properties.

The rotors, both LP and HP, were modeled as a beam using BAR elements with concentrated mass equivalent to blades and disks. Non-structural parts with considerable mass such as an accessary gear box and other equipment were modeled with CONM2 cards. Fig. 1 also shows a final FEM model which has about 1,500 grid points and 2,300 elements. The model was supported at engine mount positions by using single point constraint function.

The loads applied to the model in a static analysis were inertia, thrust distribution and intake lift. Absolute values of the loads corresponding to typical flight cases were provided by airframe manufacturers. Therefore NASTRAN calculations were carried out for unit load cases and final results were provided by a post-processor considering the load factors for the typical flight cases.

The distributed gravity load was calculated within NASTRAN using the GRAV card. The thrust load which could be regarded as distributed load on the casing was modeled as appropriate grid point forces in the axial direction. Intake lift, which was generated by external aerodynamics loads on the intake structure, was modeled as circumferentialy distributed grid point forces around an assumed intake structure model.

Since engine performance depends on maintaining tight running clearances between rotors and casings, rubbing between them increases clearance and decreases engine efficiency in respect of specific fuel consumption. Superposing the calculated results of the unit load case multiplied by the load factors, casing radial deflections relative to the rotor are obtained for various flight cases including take-off, vertical gust, lateral gust, heavy landing and so on. These deflections are compared with the base line data, in case of pass off test condition in order to estimate the largest tip clearance change. Since the decrease in the component efficiency is provided as a function of tip clearance change, each component efficiency reduction can be calculated using the estimated tip clearance increase due to rubbing. Therefore, the performance deterioration of the engine can be estimated as % increase in SFC by means of a performance influence coefficient of each component.

Further refinments of the analytical procedure with regard to the estimation of the engine performance deterioration will be accomplished in the future by actual engine tests.

RESULTS

Calculation results are illustrated in the following.

Vertical sectional deformation plots are shown in Fig. 2 using the standard routine built in NASTRAN plot capability with the PLOTEL cards. Since the intertia of an intake, and equipment on the fan casing is large, the fan casing inclines downwards under unit downward gravity load as shown in Fig. 2.1. This deflection could be seen more clearly in the center-line deflections as shown in Fig. 3.

Horizontal sectional deformation under sideward gravity load is shown in Fig. 2.2. The engine casing with rotor moves sidewards because the line from the front mount to the rear mount position does not coincide with but is located above the engine center-line. The deformation under thrust load distribution is shown in Fig. 2.3. Engine moves forwards and moreover the fan casing inclines upwards owing to the pitch moment caused by the eccentricity of the thrust mount position to the engine center line.

Fig. 2.4 shows the deformation in the vertical section under intake lift load. Larger displacements could be seen at the fan casing where intake lift is loaded.

Relative radial deflection of the casings to the rotors are shown in Fig. 4. In the case of downward gravity load, large inward deflection occurs at the top of the fan casing, while it occurs at the bottom of the core casing because of HP rotor bending.

Fig. 4.2 indicates that, the probability of tip rubbing is higher at the bottom in the fan but at the top in the HP compressor and besides at the sides in the turbine under intake lift load. There are two kinds of deformations which cause tip rubbing. One is bending deflection difference between casings and rotors. The other is oval deformation in the casing cross section. Three dimensional finite element analysis is required so as to analyze both deformations simultaneously.

Equivalent stress contour maps in the core casing is shown in Fig. 5 using NASTRAN plot capability. The stress level is far below the criteria in the case of vertical gravity load.

Fig. 6 provides intermediate casing strut stress distributions under vertical gravity load. Since this component is not only complicated but required high structural integrity, a more precise model was made for detail strength analysis as shown in Fig. 7.

CONCLUSION

NASTRAN is available for engine carcass deflection analysis using overall structural model as well as stress analysis for each components. We can use these analytical results for optimizing engine geometrical configuration in order to achieve weight reduction while maintaining high performance.

ACKNOWLEDGEMENTS

The authors are indebted to Mr. P. B. Blackman, Mr. R. Williams and Mr. B. Woolfries in Rolls-Royce Limited for their technical advices.

REFERENCES

1) E. G. Stakolich et al : Effect of Flight Loads on Turbo-fan Engine Performance Deterioration, NASA TM-79041 (1979)

2) E. G. Stakolich and W. J. Stromberg : JT9D Performance Deterioration Results from a Simulated Aerodynamics Load Test, AIAA/SAE/ASME 17th Joint Propulsion Conf., (July, 1981)

3) J. L. White and E. S. Todd : Normal Modes Vibration Analysis of the JT9D/747 Propulsion System, Journal of Aircraft, Vol. 15, No. 1 pp. 28 - 32, (Jan., 1978)

4) J. L. White and D. L. Beste : Nastran Application to Aircraft propulsion Systems Proc. 4th MSC / NASTRAN Users' Conf., pp. 91 - 96, (Sept., 1975).

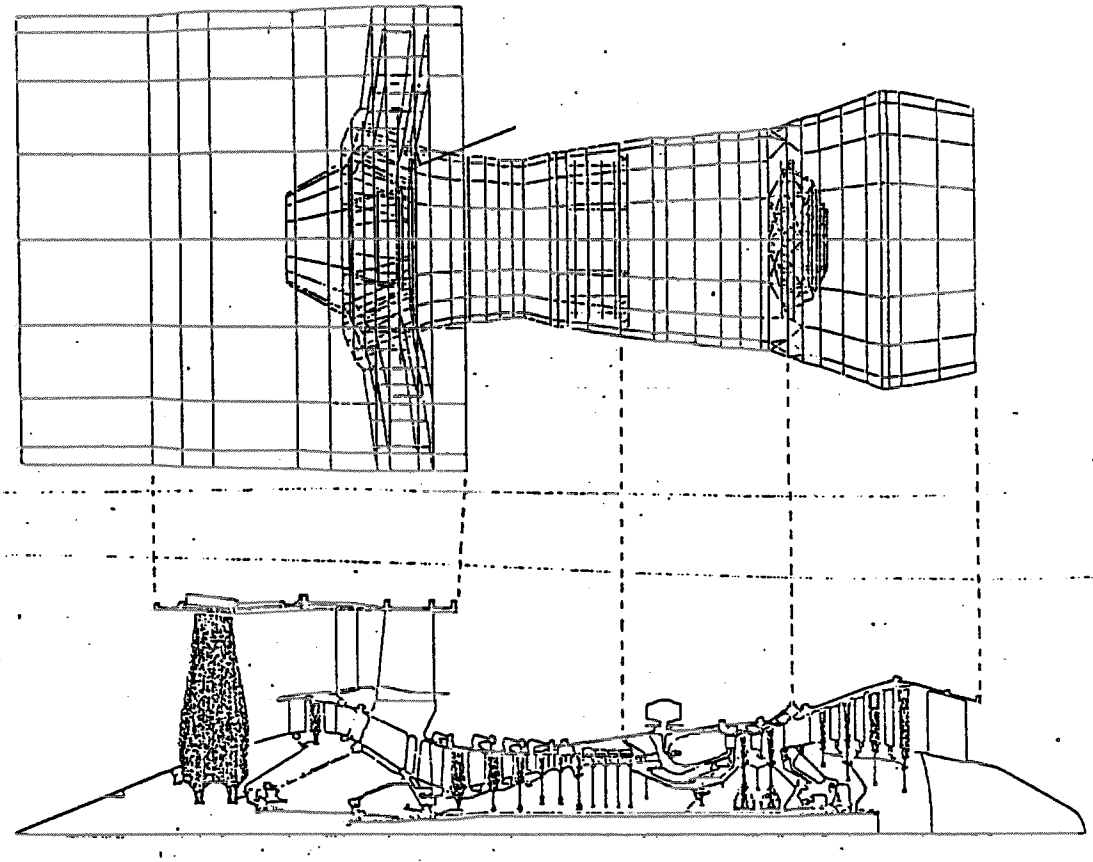

FIG.1 General Arrangement and Structural Model

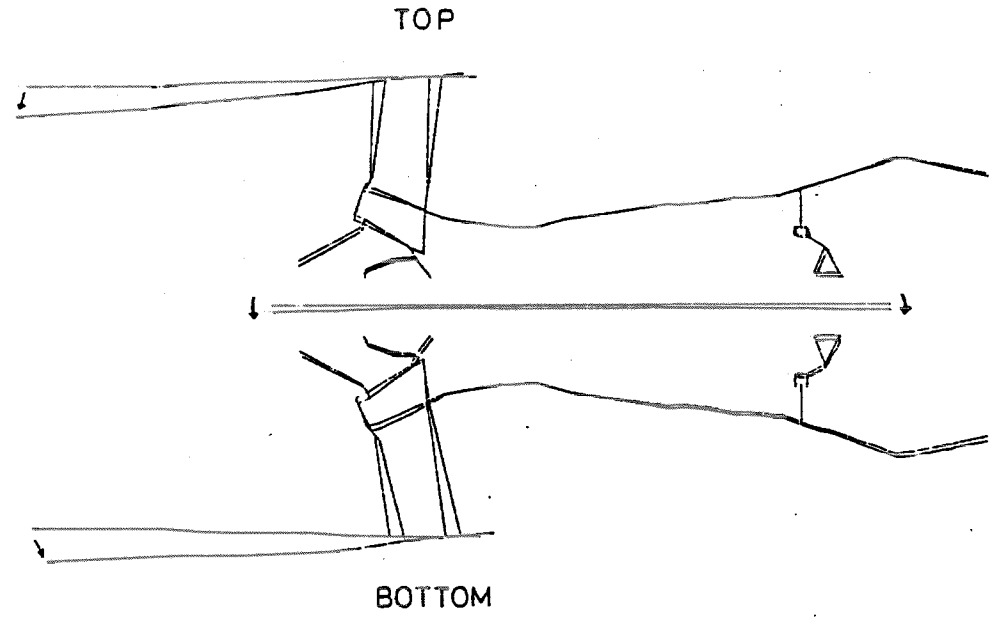

FIG.2.1 Vertical Sectional Deformation
in the case of Downward Gravity Load

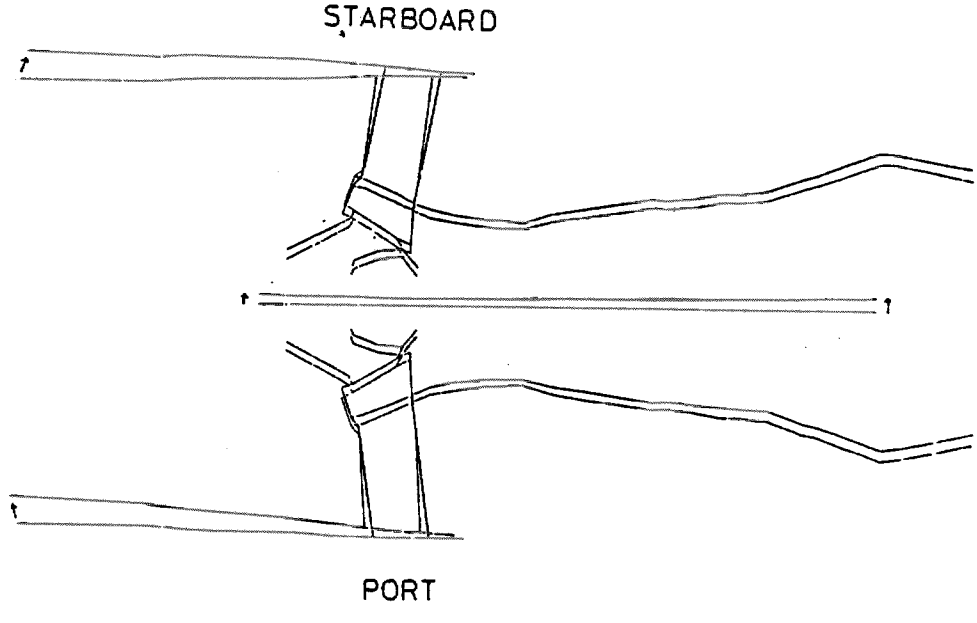

FIG.2.2 Horizontal Sectional Deformation
in the case of Sideward Gravity Load

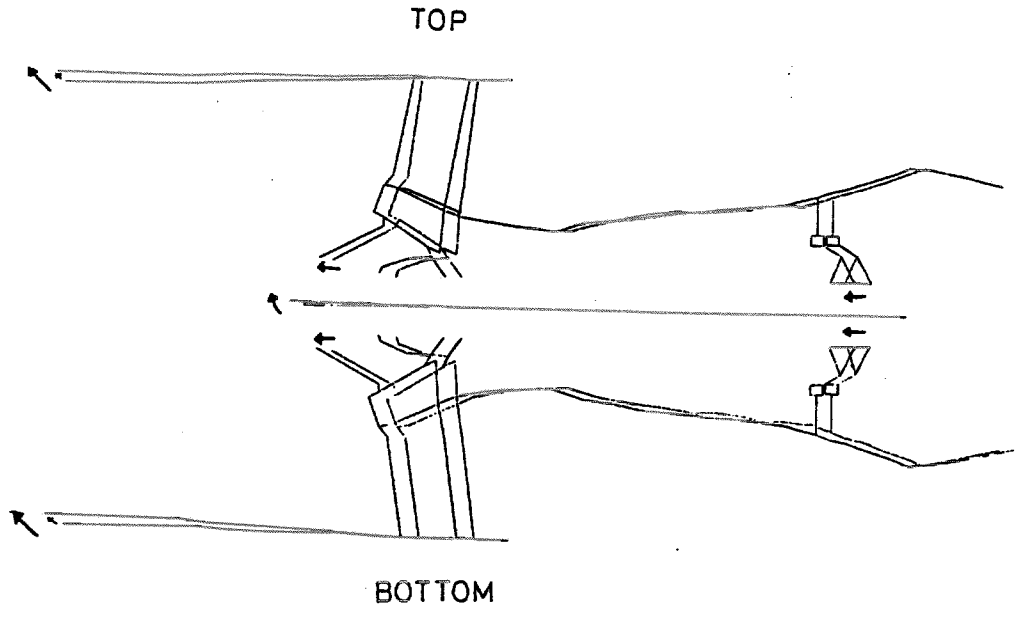

FIG.2.3 Vertical Sectional Deformation in the case of Thrust Load

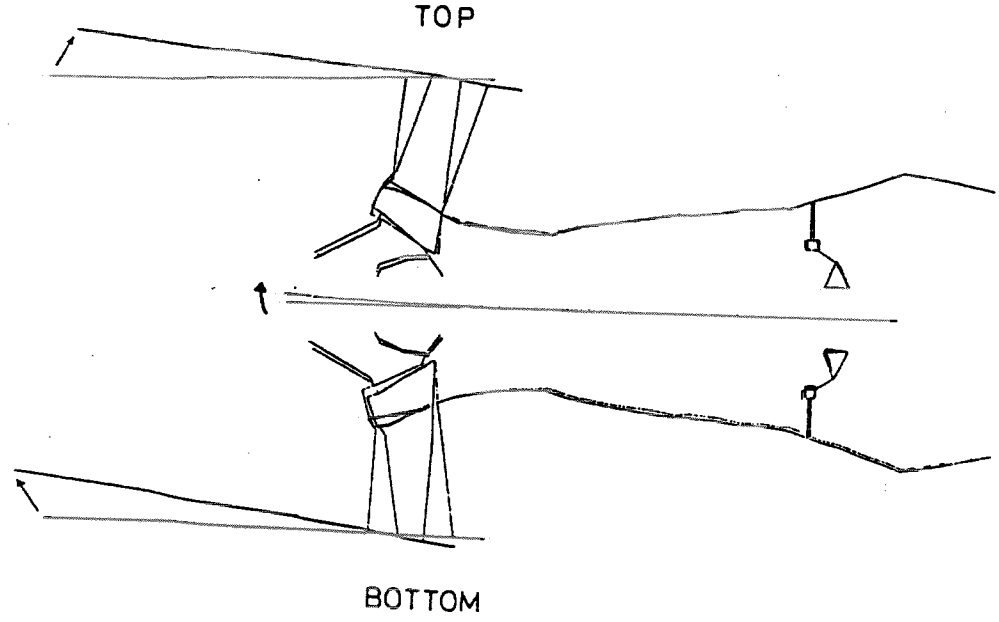

FIG.2.4 Vertical Sectional Deformation in the case of Intake Lift Load

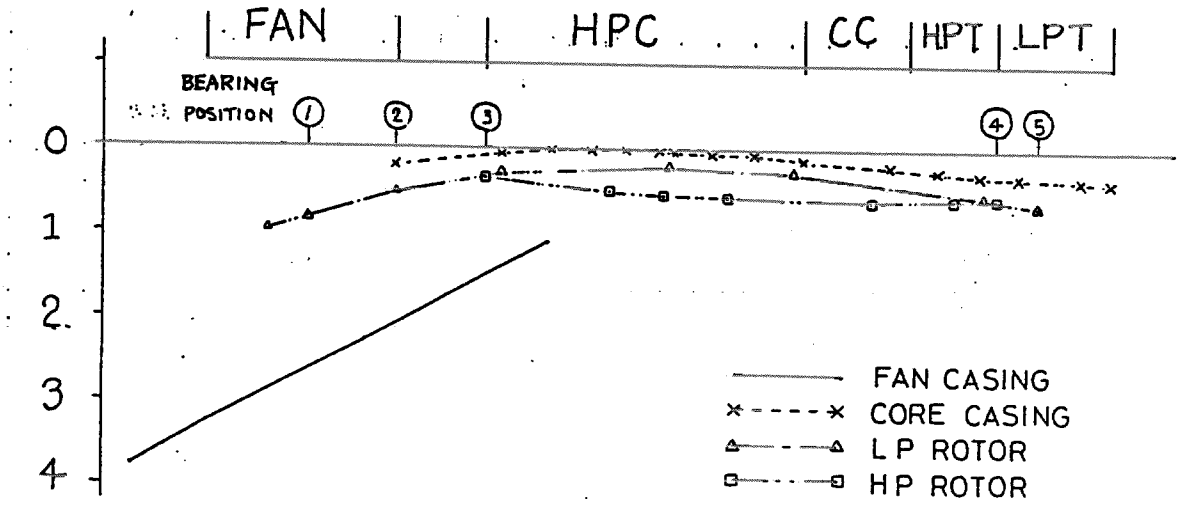

FIG.3 Deflection Lines in the case of Downward Gravity Load

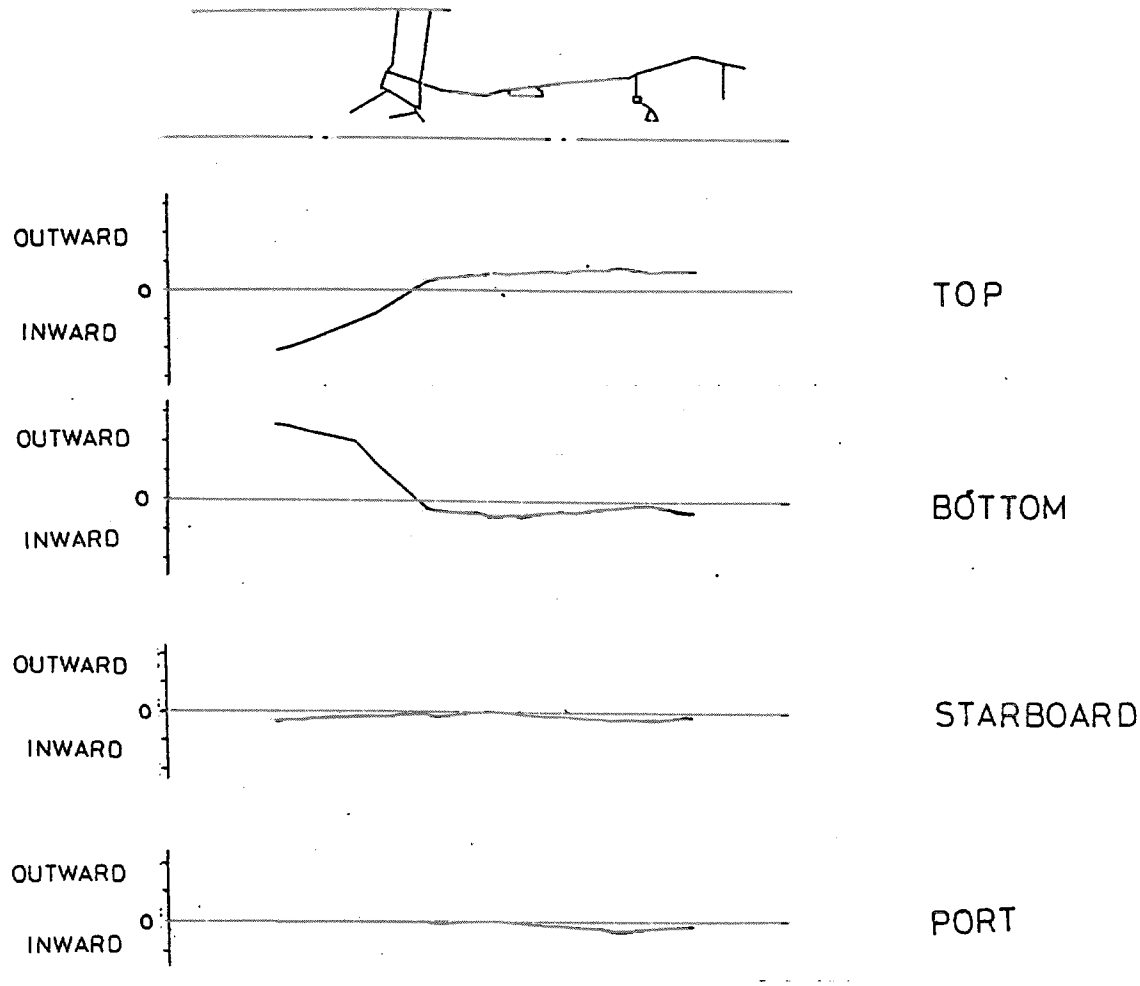

FIG.4.1 Casing Relative Deflection to Rotor in the case of Downward Gravity Load

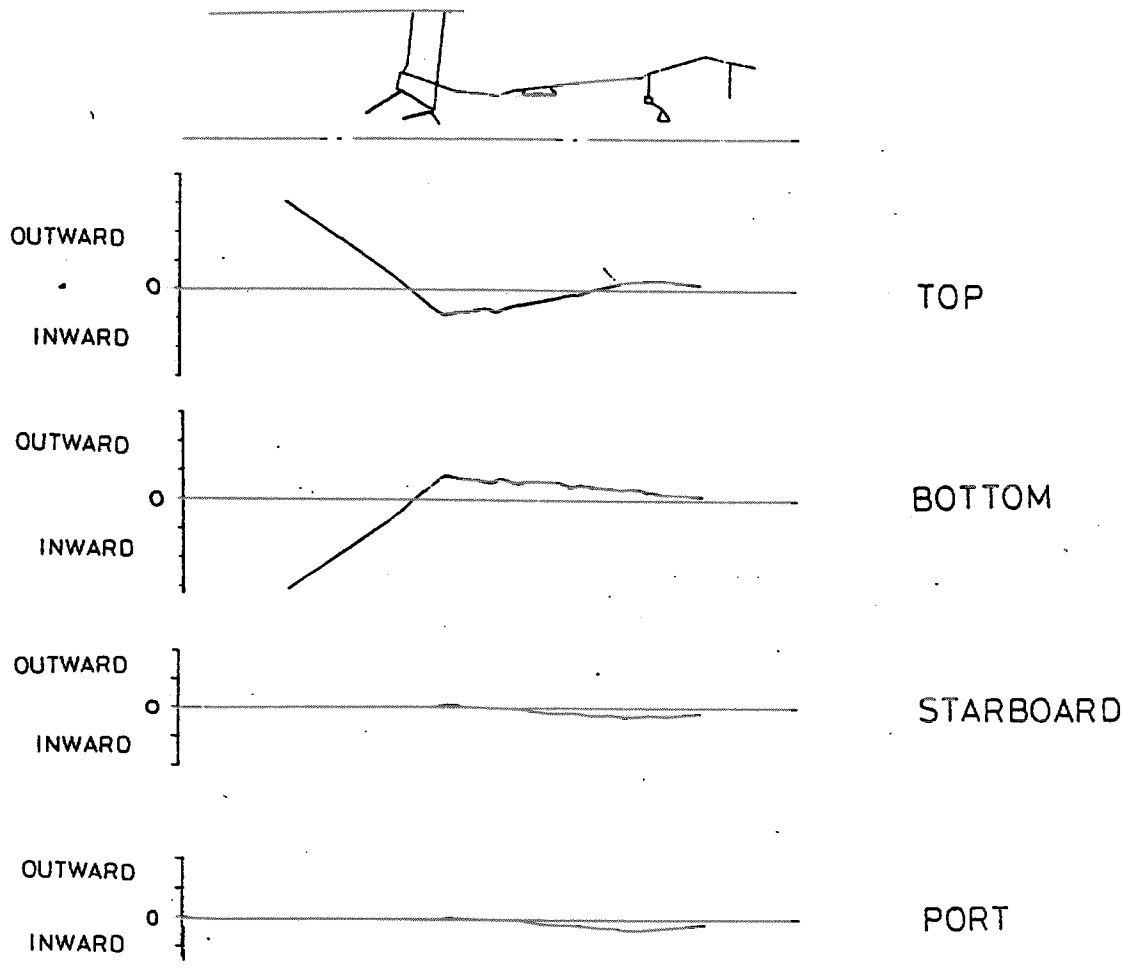

FIG.4.2 Casing Relative Deflection to Rotor
in the case of Intake Lift Load

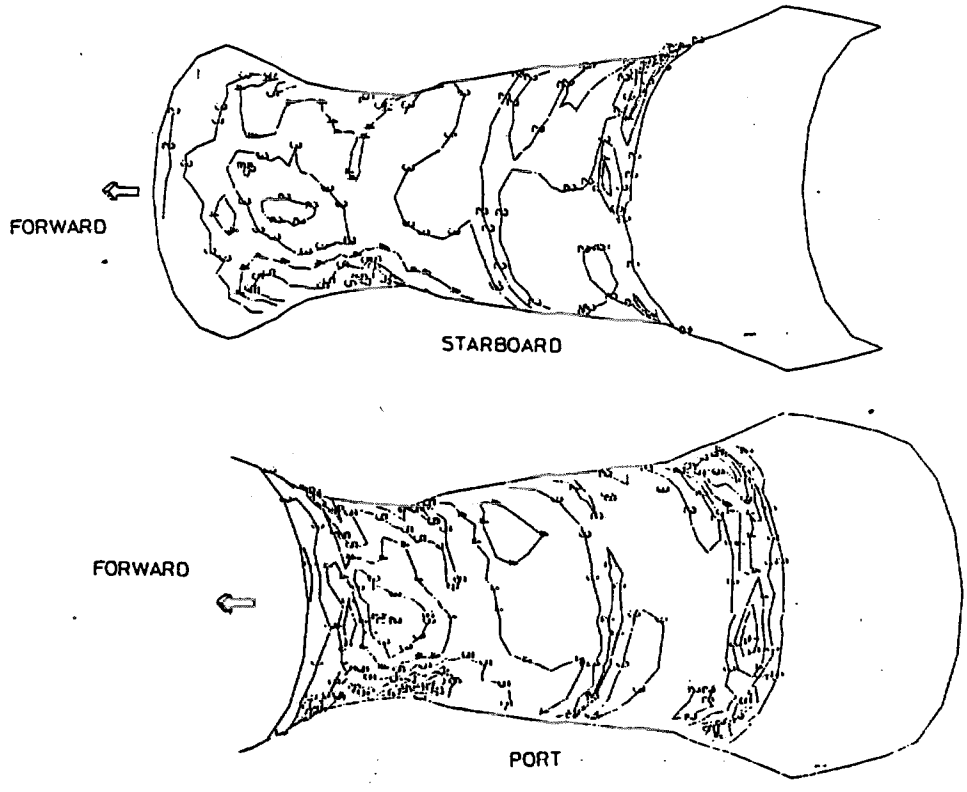

FIG.5 Stress Distribution on Casing in the case of Downward Gravity Load

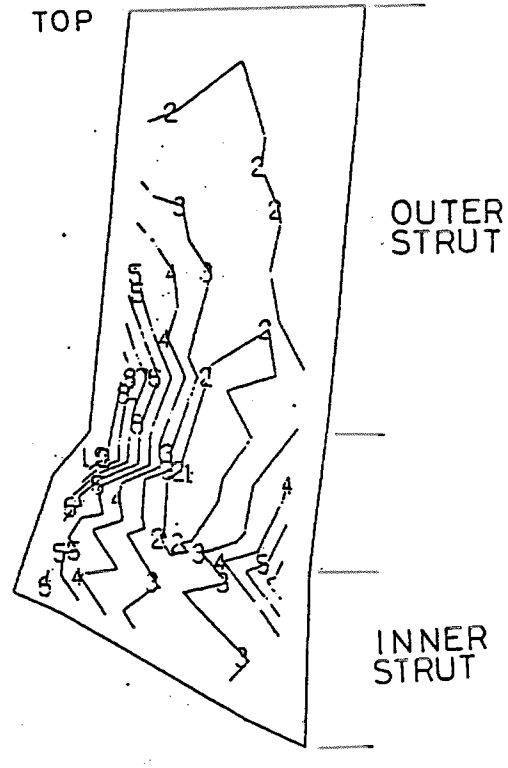

FIG.6 Stress Distribution on Intermediate Casing Strut in the case of Downward Gravity Load

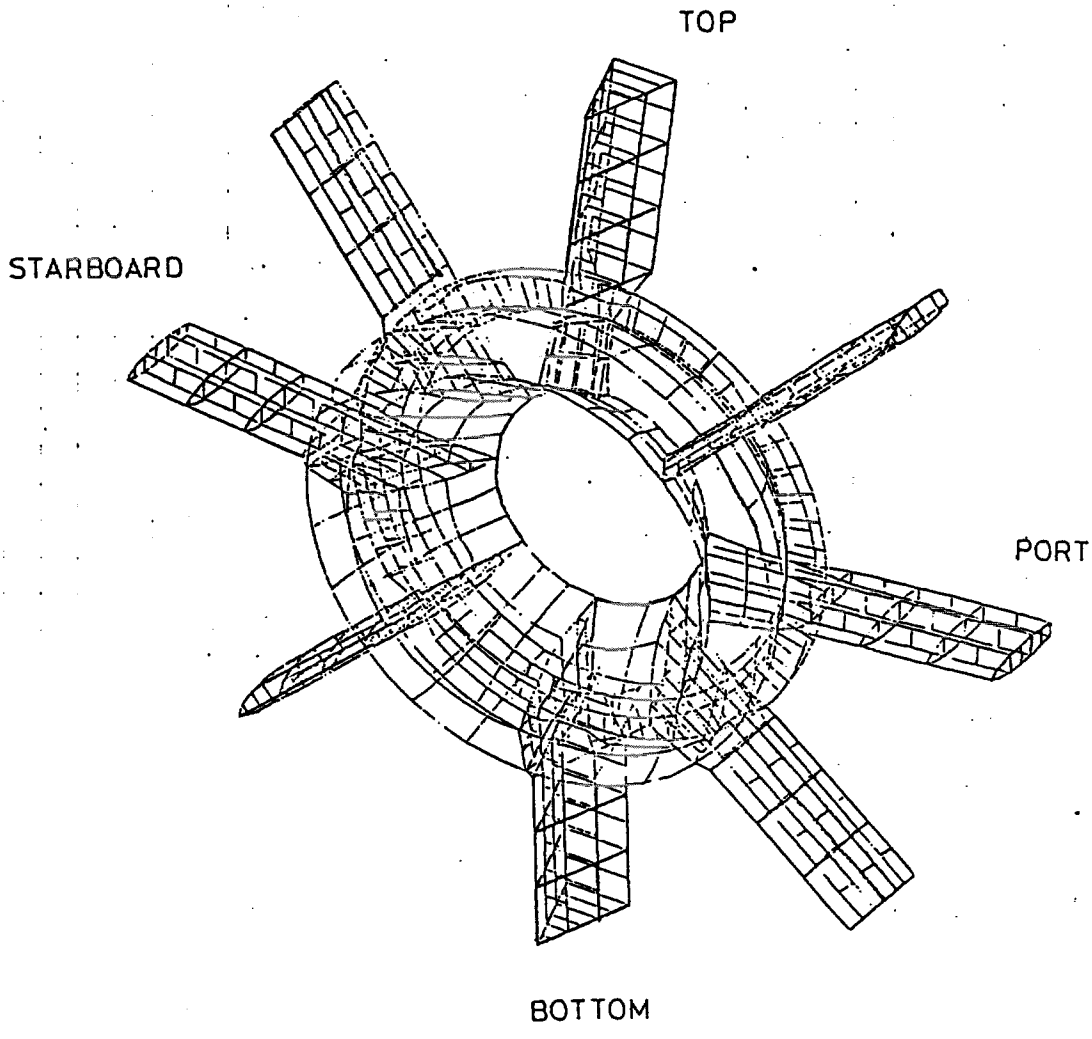

FIG.7 Intermediate Casing Stress Analysis Model